ARTICLE IN PRESS – Acta Cryst. B

STRUCTURAL SCIENCE
CRYSTAL ENGINEERING
MATERIALS

ISSN 2052-5206

Br···Br and van der Waals interactions along a homologous series: crystal packing of 1,2-dibromo-4,5-dialkoxybenzenes

Proof instructions

Proof corrections should be returned by **5 August 2016**. After this period, the Editors reserve the right to publish your article with only the Managing Editor's corrections.

Please
(1) Read these proofs and assess whether any corrections are necessary.
(2) Check that any technical editing queries highlighted in **bold underlined** text have been answered.
(3) Send corrections by e-mail to **jb@iucr.org**. Please describe corrections using plain text, where possible, giving the line numbers indicated in the proof. Please do not make corrections to the pdf file electronically and please do not return the pdf file. If no corrections are required please let us know.

If you wish to make your article **open access** or purchase printed offprints, please complete the attached order form and return it by e-mail as soon as possible.

Please check the following details for your article

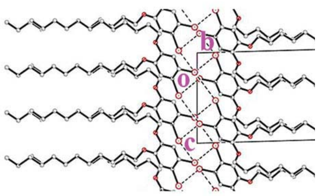

Thumbnail image for contents page

Synopsis: The crystalline structures of four homologues of the 1,2-dibromo-4,5-dialkoxybenzene series [$Br_2C_6H_2(OC_nH_{2n+1})_2$ for n = 2, 12, 14 and 18] have been solved by means of single-crystal crystallography.

Abbreviated author list: Suarez, S.A.; Muller, F.; Gutiérrez-Suburu, M.E.; Fonrouge, A.; Baggio, R.F.; Cukiernik, F.D.

Keywords: chemical crystallography; 1,2-dibromo-4,5-dialkoxybenzenes; halogen bonds; crystal engineering

PLEASE PROVIDE NEW SQUARE-SHAPED THUMBNAIL WITH LESS TEXT

How to cite your article in press

Your article has not yet been assigned page numbers, but may be cited using the doi:

Suarez, S.A., Muller, F., Gutiérrez-Suburu, M.E., Fonrouge, A., Baggio, R.F. & Cukiernik, F.D. (2016). *Acta Cryst.* B**72**, doi:10.1107/S2052520616009835.

You will be sent the full citation when your article is published and also given instructions on how to download an electronic reprint of your article.

Acta Cryst B
STRUCTURAL SCIENCE
CRYSTAL ENGINEERING
MATERIALS

ISSN 2052-5206

Received 22 April 2016
Accepted 16 June 2016

Edited by J. Lipkowski, Polish Academy of Sciences, Poland

Keywords: chemical crystallography; 1,2-dibromo-4,5-dialkoxybenzenes; halogen bonds; crystal engineering.

CCDC references: 1486248; 1486249; 1486250; 1486251

Supporting information: this article has supporting information at journals.iucr.org/b

Br···Br and van der Waals interactions along a homologous series: crystal packing of 1,2-dibromo-4,5-dialkoxybenzenes

Sebastián A. Suarez,[a,b] Federico Muller,[a] Matías E. Gutiérrez-Suburu,[a] Ana Fonrouge,[a] Ricardo F. Baggio[b]* and Fabio D. Cukiernik[a]*

[a]INQUIMAE, Departamento de Química Inorgánica, Analítica y Química Física, Facultad de Ciencias Exactas y Naturales, Universidad de Buenos Aires, Ciudad Universitaria, Pab. II (1428), Buenos Aires, Argentina, and [b]Gerencia de Investigación y Aplicaciones, Centro Atómico Constituyentes, Comisión Nacional de Energía Atómica, Buenos Aires, Argentina. *Correspondence e-mail: baggio@tandar.cnea.gov.ar, fabioc@qi.fcen.uba.ar

The crystalline structures of four homologues of the 1,2-dibromo-4,5-dialkoxybenzene series [$Br_2C_6H_2(OC_nH_{2n+1})_2$ for n = 2, 12, 14 and 18] have been solved by means of single-crystal crystallography. Comparison along the series, including the previously reported n = 10 and n = 16 derivatives, shows a clear metric trend (**b** and **c** essentially fixed along the series and **a** growing linearly with n), in spite of some subtle differences in space groups and/or packing modes. A uniform packing pattern for the aliphatic chains has been found for the n = 12 to 18 homologues, which slightly differs from that of the n = 10 derivative. The crystalline structures of all the higher homologues (n = 10–18) seem to arise from van der Waals interchain interactions and, to a lesser extent, type II Br···Br interactions. The dominant role of interchain interactions provides direct structural support for the usual interpretation of melting point trends like that found along this series. *Atoms in Molecules* (AIM) analysis allows a comparison of the relative magnitude of the interchain and Br···Br interactions, an analysis validated by the measured melting enthalpies.

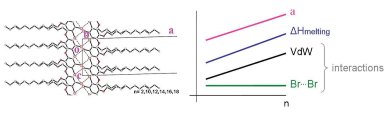

1. Introduction

The crystalline structures of molecular compounds arise from the optimization of attractive and repulsive interactions (Dunitz & Gavezzotti, 1999). Attractive interactions involve both isotropic and strongly directional ones (Desiraju, 2013) like the whole palette of hydrogen bonds (Steiner, 2002; Desiraju, 2002), $\pi\cdots\pi$ interactions (Martinez & Iverson, 2012), C—H···π interactions (Nishio, 2004), halogen bonds (Cavallo *et al.*, 2016), *inter alia*.

These interactions may also be at the origin of specific physical properties of the compounds, like magnetic behaviour (Iwasaki *et al.*, 1999), optoelectronic properties (**Zang, 2008 [not in ref. list?]**) or melting points (Bekö *et al.*, 2014; Joseph *et al.*, 2011).

Non-covalent interactions may act either in competitive or synergistic fashions, especially in the case of multiblock molecular compounds. Homologous series of compounds represent an interesting case in this context, as van der Waals interactions between aliphatic chains increase progressively as the chain length – usually quantified as the number of C atoms in each chain, n – increases.

Very often melting points of homologous series decrease up to a certain n value, then increase with n up to a saturation value (a 'fall–rise' trend). The same kind of behavior has been found for glass transition temperatures of side-chain polymers (Platé & Shibaev, 1974) and transition temperatures of liquid crystals (Ibn-Elhaj *et al.*, 1992; Demus *et al.*, 1998). It is usually interpreted that, for long aliphatic chains, their packing is the main driving force for the crystal structure; in these cases, the other molecular block acts as a disturbing agent for the packing, this effect being stronger (lower m.p.) as chain length decreases. For short aliphatic chains, the structure arises from the packing requirements of the other molecular block; increasing chain length progressively disturbs this packing, facilitating the melting process.

Experimental bases for this argument often come from indirect structural information, such as powder X-ray diffraction experiments. We recently provided direct structural evidence for such behaviour, through detailed crystalline structures solved by single-crystal crystallography (Cukiernik *et al.*, 2008; Fonrouge *et al.*, 2013). Indeed, for 1,2-dibromo-4,5-dialkoxybenzenes (Scheme 1), a homologous series exhibiting the already described 'fall-rise' m.p. *versus* *n* trend (Fig. 1), we have shown that the structure of the $n = 1$ homolog is governed by $\pi\cdots\pi$, dipolar and Br$\cdots$O halogen-bond interactions, whereas those of the higher homologs with $n = 10$ and 16 are dominated by van der Waals interactions between the aliphatic chains. We also pointed out some minor differences between the structures of the $n = 10$ and $n = 16$ derivatives (hereinafter N10 and N16): in the first case, the molecules are organized through type II Br$\cdots$Br interactions (see below for a description of such interactions) giving rise to head-to-head dimers; in the second case, the organization does not involve such dimers but is better described as head-to-tail, involving Br$\cdots\pi$ interactions.

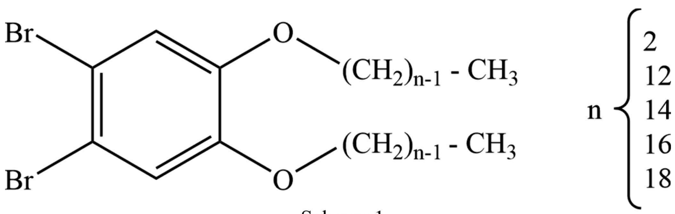

Scheme 1

We thus decided to extend our study to other members of this series, in order to test the validity of the 'diblock argument' on the melting points trend and additionally to detect if a transition from head-to-head to head-to-tail organization operates for a specific *n* value. In this work we report the crystalline structures of the $n = 2$, 12, 14 and 18 members of the 1,2-dibromo-4,5-dialkoxyebnzene series (hereinafter N02, N12, N14 and N18) and perform a comparative analysis of the structures of its higher homologs ($n = 10$, 12, 14, 16 and 18). Through this analysis, we compare their crystallographic characteristics and interpret their thermal behaviour (melting points and enthalpies) in terms of the magnitude of the non-covalent interactions, analyzed both in terms of the crystallographic distances and through the Atoms in Molecules (AIM) theory (Bader, 1990).

2. Experimental

A Carlo Erba EA1150 elemental analyser was used for microanalysis (*Servicio a Terceros*, INQUIMAE). ^{1}H NMR spectra were recorded (at UMYMFOR-FCEN-UBA) on a Bruker AM500 spectrometer, using $CDCl_3$ as a solvent and its residual peaks as internal references (7.26 p.p.m. for ^{1}H). Differential scanning calorimetry (DSC) on individual single crystals was performed with a Shimadzu DSC-50 apparatus. Single-crystal X-ray diffraction data were collected using a Gemini diffractometer (Oxford Diffraction). Measurements were performed at 298 K **[Does not match value in Table 1]**. Data collection strategy and data reduction followed standard procedures implemented in *CrysAlisPro* software (Oxford Diffraction, 2009 **[changed ref. – OK?]**).

2.1. Synthesis, characterization and crystallization

All the studied compounds were synthesized from catechol in two steps, as previously reported (Fonrouge *et al.*, 2013), except for N02, synthesized by bromination of commercial 1,2-diethoxybenzene. The first synthetic step involves the Williamson etherification of catechol with the corresponding bromoalkane; the second one, the controlled bromine addition in the activated *p*-positions to the alkoxy chains. The synthetic procedure for N14 is described in detail below, as an example.

In a three-necked flask equipped with a glycerine bubbler, cathechol (1.129 g) was dissolved under stirring in butanone (7 ml), then finely divided anydrous K_2CO_3 (4.08 g previously dried for 2 h at 393 K) was added. After the addition of an additional 3 ml of butanone under Ar flow, the reaction mixture was heated to reflux, then 14-bromotetradecane (6.5 ml) dissolved in butanone (3 ml) was added. The reaction was monitored by thin layer chromatography (TLC, cyclohexane:dichloromethane 3:1 v/v) up to completion, then allowed to cool to room temperature. The crude solid was filtered then dissolved in dichloromethane and finally extracted with HCl 10% m/v. After drying the organic phase with anhydrous Na_2SO_4, the mixture was filtered off then the solution was dried under vacuum. The solid 1,2-di(te-

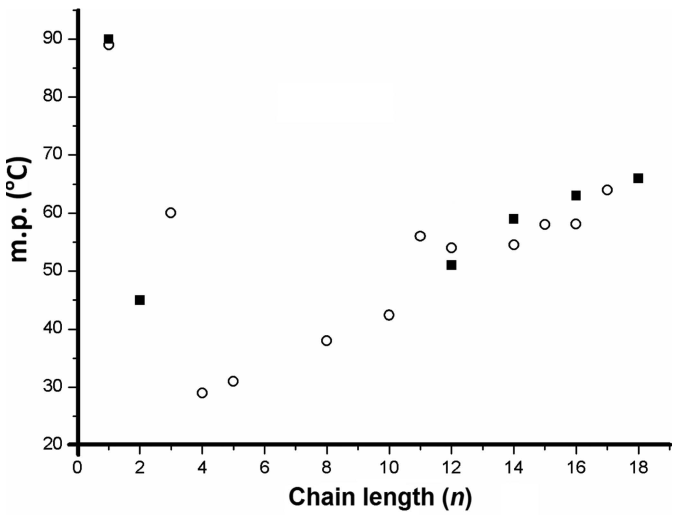

Figure 1
Melting points for the 1,2-dibromo-4,5-dialkoxybenzene series. Open circles: already reported data for powdered compounds; filled squares: measured values for structures solved by single-crystal methods.

tradecyloxy)benzene was further purified by column chromatography (silica gel 60, cyclohexane to cyclohexane:dichloromethane 95:5 as elution solvent). Bromination was achieved by dissolving the obtained 1,2-di(tetradecyloxy)benzene (0.553 g) in cold CH_2Cl_2 (8 ml), placing the solution in a two-necked flask equipped with an $NaHSO_3$ bubbler with pressure compensation and immersed in an ice bath. Bromine (0.1 ml) dissolved in CH_2Cl_2 (2 ml) was added dropwise and the mixture was allowed to warm to room temperature. The progress of the reaction was monitored by TLC (CH_2Cl_2–cyclohexane, 1:3 v/v). When the reaction was complete, it was quenched by the addition of aqueous $NaHSO_3$. The aqueous phase was discarded and the organic phase was washed successively over water, aqueous $NaHSO_3$ and water, then dried with anhydrous Na_2SO_4, filtered and evaporated to dryness in a rotary evaporator. The solid was recrystallized from ethanol. Overall yield: 0.610 g (9%). Elemental analysis: exp. (calc.): C: 61.2 (61.8), H: 8.6 (9.15)%. ^{1}H NMR: δ 7.1 (s, 2H), δ 3.9 (t, 4H), δ 1.8 (q, 4H), δ 1.3 (m, 44H), δ 0.9 (m, 6H).

For N02: diethoxybenzene 0.912 g, yield: 1.274 g (71%). Recrystallized from water. Elemental analysis: exp. (calc.): C: 37.2 (37.1), H 3.8 (3.7)%. ^{1}H NMR: δ 7.1 (s, 2H), δ 4.1 (q, 4H), δ 1.4 (t, 6H). For N12: cathechol 2.989 g, bromododecane 15.4 ml, yield: 0.405 g (25%). Elemental analysis: exp. (calc.): C 55.0 (59.6), H 8.2 (8.7)%. ^{1}H NMR: δ 7.1 (s, 2H), δ 3.9 (t, 4H), δ 1.8 (q, 4H), δ 1.3 (m, 37H), δ 0.9 (m, 6H). For N18: cathechol 0.508 g, bromooctadecane: 3.681 g, yield: 0.317 g (11%). Elemental analysis: exp. (calc.): C 64.9 (65.3), H 10.1 (9.9)%. ^{1}H NMR: δ 7.06 (s, 2H), δ 3.94 (t, 4H), δ 1.79 (q, 4H), δ 1.44 (q, 4H),δ 1.29–1.23 (m, 56H), δ 0.88 (t, 6H).

Single crystals of N02, N12 and N14 were obtained by slow evaporation from concentrated solutions at room temperature. Crystals used for data collection and refinement were those grown from toluene (N12), cyclohexane (N14) and ethanol (N02). Crystals of N02 grown from methanol and from cyclohexane were checked for their cell parameters, which were identical to those obtained from ethanol; crystals of N12 grown from cyclohexane were identical to those grown from toluene. Single crystals of N18 were obtained by slow evaporation from an *n*-heptane solution.

2.2. Crystal structure resolution and refinement

The crystal structures were solved by direct methods (*SHELXS*97; Sheldrick, 2008) and refined by least squares on F^2 (*SHELXL*2014/6; Sheldrick, 2015). All C, H atoms were identified in an intermediate difference map, further idealized and finally refined as riding; their displacement parameters taken as $U_{\rm iso}({\rm H}) = xU_{\rm eq}({\rm C})$, with C—H = 0.93 Å and $x = 1.2$ for aromatic, C—H = 0.97 Å and $x = 1.2$ for methylene and C—H = 0.96 Å and $x = 1.5$ for methyl groups.

3. Molecular calculations

3.1. AIM: brief theoretical background

The quantum theory of *Atoms in Molecules* (AIM) provides an approach to the analysis of the electron density distribution of a molecule, an experimental observable, based on its topology. Each point in space is characterized by a charge density $\rho(r)$, and further quantities such as: the gradient of $\rho(r)$, the Laplacian functions of $\rho(r)$, and the matrix of the second derivatives of $\rho(r)$ (Hessian matrix). The magnitudes of the density at the critical points give a measure of bond order and interaction strength and can be used to assess, at least in comparative terms, the real significance of some non-covalent interactions, usually evaluated only on geometrical

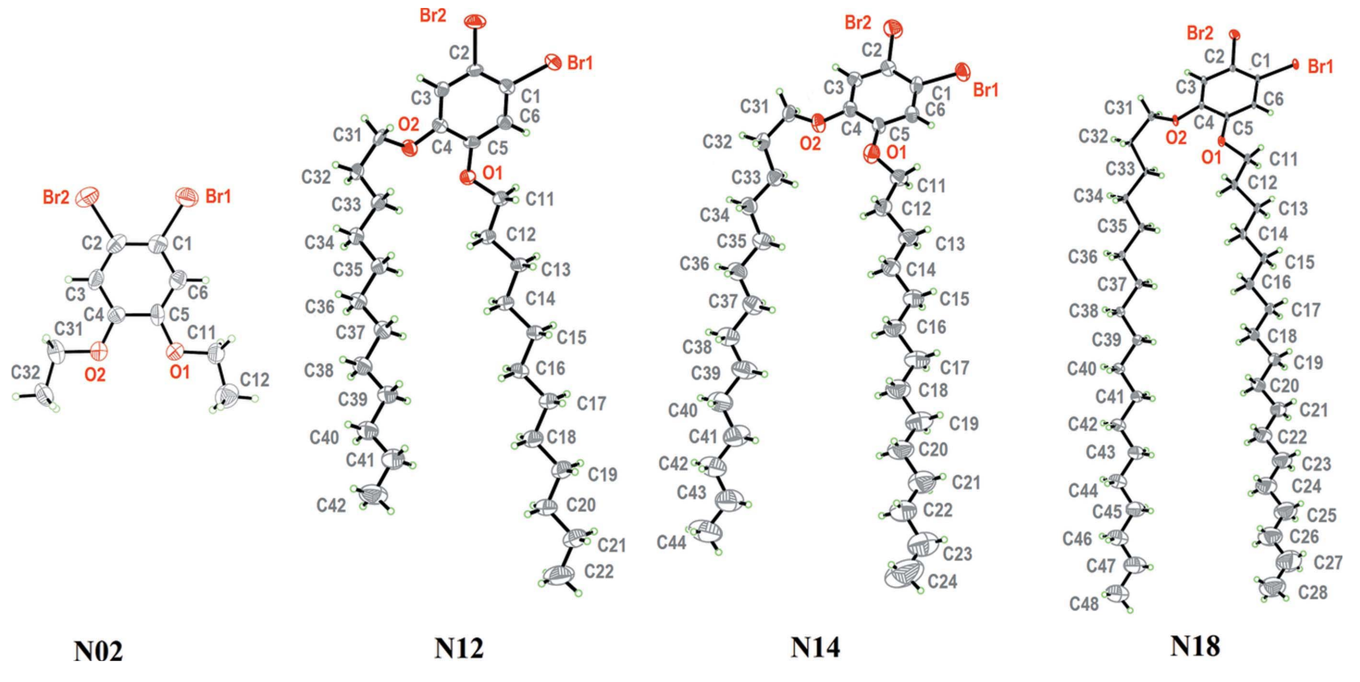

Figure 2
Ellipsoid plots (at athe 40% probability level) for N02, N12, N14 and N18.

Table 1
Experimental details.

ϕ: angle between Br---Cg and the plane normal.

	N01[a]	N02[b]	N10[c]	N12[b]	N14[b]	N16[c]	N18[b]
Chemical formula	$C_8H_8Br_2O_2$	$C_{10}H_{12}Br_2O_2$	$C_{26}H_{44}Br_2O_2$	$C_{30}H_{52}Br_2O_2$	$C_{34}H_{60}Br_2O_2$	$C_{38}H_{68}Br_2O_2$	$C_{42}H_{76}Br_2O_2$
M_r	295.96	324.02	548.43	604.53	660.64	716.72	772.84
Crystal system, space group	Triclinic, $P\bar{1}$	Monoclinic, $P2_1/c$	Monoclinic, $C2/c$	Monoclinic, $P2_1/c$	Monoclinic, $P2_1/c$	Monoclinic, Cc	Monoclinic, $C2/c$
Temperature (K)	294	294	150	294	294	294	294
a, b, c (Å)	10.1170 (5), 10.2052 (5), 20.2764 (10)	16.663 (6), 7.943 (5), 8.924 (5)	67.0788 (15), 4.47170 (10), 18.2399 (4)	39.897 (6), 8.421 (4), 9.321 (5)	45.220 (7), 8.374 (4), 9.279 (4)	50.158 (5), 8.360 (4), 9.248 (4)	110.750 (5) 8.2292 (3) 9.1539 (3)
α, β, γ (°)	104.1710 (12), 98.9405 (10), 101.0630 (12)	90, 94.725 (5), 90	90, 101.216 (2), 90	90, 91.622 (5), 90	90, 91.809 (5), 90	90, 94.136 (5), 90	90, 92.268 (2), 90
V (Å^3)	1946.46 (17)	1177.1 (11)	5366.7 (2)	3130 (3)	3512 (3)	3868 (2)	8336.2 (5)
Z	8	4	8	4	4	4	8
μ (mm^{-1})	8.29	6.86	3.04	2.61	2.33	2.13	1.976
D_x (g cm^{-3})	2.020	1.828	1.358	1.283	1.249	1.231	1.232
$R[F^2 > 2\sigma(F^2)]$, $wR(F^2)$, S	0.0356, 0.0966, 1.015	0.0774, 0.2646, 0.967	0.1237, 0.3290, 1.165	0.0929, 0.2304, 1.053	0.1074, 0.3195, 1.035	0.0240, 0.0516, 0.841	0.1132, 0.1329, 1.129
$d_{\rm Br---Br}$ (Å) (dimeric)	–	3.764	3.644	3.696	3.707	–	3.675
$d_{\rm Br---Br}$ (Å) (interdimeric)	(3.72)	3.694	3.870	3.745	3.736	–	3.688
$d_{{\rm Br---}Cg}$(Å)/ϕ°	–	–	4.18/41.6	4.03/13.0	4.01/12.4	3.98/10.3	3.943 (4)/10.2

References: (*a*) Cukiernik *et al.* (2008); (*b*) this work; (*c*) Fonrouge *et al.* (2013).

grounds (Bader, 2009). Some critical viewpoints concerning the application of this method when *absolute* AIM values are analyzed have recently been raised (Spackman, 2015); neverthless, its use for *relative comparisons* is still growing (Wang *et al.*, 2016).

3.2. Programs used and approximations performed

Quantum-mechanical calculations on the complexes included in this study were performed at the M062X/6-311++G(d,p) level of theory using the crystallographic coordinates (single-point calculations) within the *GAUSSIAN*09 program (Frisch *et al.*, 2009). This functional/basis set combination has proven to be adequate to explore other related systems exhibiting halogen bonds (Raffo *et al.*, 2016; Rosokha *et al.*, 2013). The basis set superposition error for the calculation of interaction energies was corrected using the counterpoise method. The AIM analysis of the electron density has been performed at the same level of theory using the *Multiwfn* program (Lu & Chen, 2012). Although charge-density calculations should preferably be performed on single-point computations based on low-temperature high-resolution crystallographic data, we are confident our *comparative* analysis is reliable, as it has been performed among structures solved under similar conditions, taking care to minimize the influence any systematic error due to its implementation could exert on the interpreted trend.

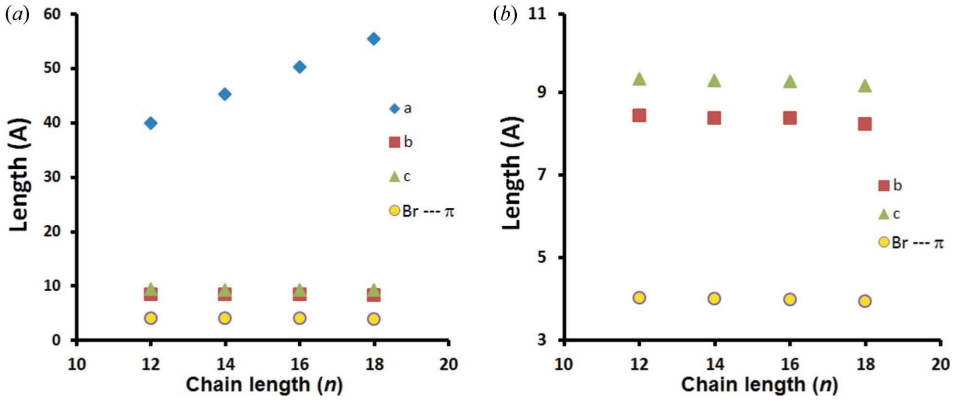

Figure 3
Dependence on chain length n of the cell parameters for the higher homologues N10–N18. (*a*) Cell parameters a, b and c. The Br$\cdots$$Cg$ distance (strictly half c) is also included. (*b*) Detail for b, c and Br$\cdots$$Cg$, showing a very slight contraction along these parameters with increasing n.

4. Results and discussion

4.1. Crystal structure

Fig. 2 shows ellipsoid plots of all four molecules reported herein, N02, N12, N14 and N18. In order to simplify future discussions, tails will be referred to as T1 and T2, being those attached to O1 and O2, respectively. Table 1, in turn, presents some relevant crystallographic and structural parameters for the molecules presented herein as well as for the already reported members of the series, N10 and N16, included for future reference. Inspection of the crystal

Files: b/lo5009/lo5009.3d b/lo5009/lo5009.sgml LO5009 FA IU-169/26(29)7 1616/8(25)7 (100) LO5009 PROOFS B:FA:2016:72:5:0:0–0

data discloses that even if with different space-group symmetries the sequence N12—N18 presents a clear metrical trend (graphically shown on Fig. 3), with values for b and c kept reasonably fixed along the series, and a growing steadily with the chain length by $\simeq 2.57$ Å per added methylene group, as expected for bilayers of extended aliphatic chains. Duplication of a in N18 is the result of the rupture of translational symmetry along this direction, and should not be interpreted as a real deviation. A more serious difference is found in the case of N10, where all three parameters depart from the trend, either by halving or duplication. This structure, however, reported in Fonrouge *et al.* (2013) was the only one measured at low temperature, data collection for the remaining ones having been performed at room temperature. This leaves room for the possible existence of a temperature-induced transformation, something we will analyze in the future, although the room-temperature XRD pattern of a powdered sample agreed with that expected from the reported low-temperature structure.

Inspection of Fig. 2 shows some of the relevant characteristics of the $n > 9$ members of the series: essentially straight tails, subtending similar angles between them (the $\langle$T1—T2$\rangle$ angular span between lines defined by their outermost C atoms being 32–37°). The packing in the group N10–N18 takes place with their tails entangled with each other in obvious manifestation of significant van der Waals interactions, a fact to be discussed below. Fig. 4 presents lateral packing views, projected along b and c (as already mentioned, tails run basically along a). In order to simplify the discussion the interacting zones (of different kinds) have been labeled as A, B, C, B′.

Zone A is common to all structures, and the dominating interactions are of van der Waals type between almost parallel aliphatic chains. Fig. 5(a) (left) shows (for N18) the particular way in which the two different types of chains **are disposed [meaning OK?]** along b: it can be seen that the independent tails T1 and T2$^{\rm i}$, (i) $x, -2-y, \frac{1}{2}+z$, lie almost parallel to each other, at a distance very near b/2, defining a plane which almost contains the [010] vector, with a deviation of less than 0.5°. The inset presents a projection down [010] showing the almost perfect overlap at the center, with minimum departure at the ends of the tails. At this stage it is worth mentioning that this description is valid for the N12 to N18 group, and is illustrated in Fig. 6(a). N10, in turn, as already mentioned, departs from the general trend and the way in which the parallel staking of tails is achieved is depicted in Fig. 6(b),

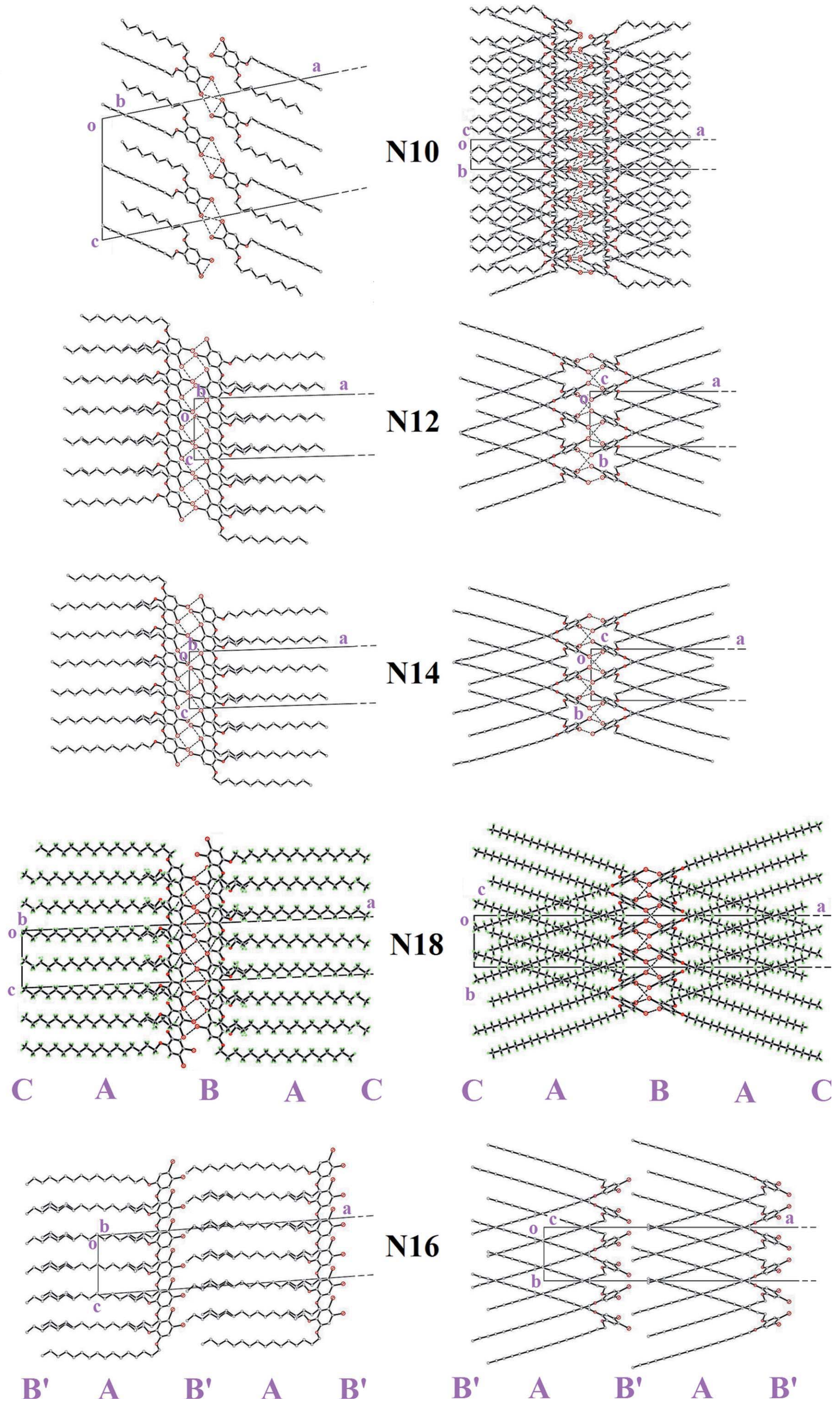

Figure 4
Lateral packing views for the $n > 2$ member of the series, projected along b and c. Labels A, B, C and B′ correspond to different interacting zones and are discussed in the text.

Files: b/lo5009/lo5009.3d b/lo5009/lo5009.sgml **LO5009** FA IU-169/26(29)7 1616/8(25)7 (100) LO5009 PROOFS B:FA:2016:72:5:0:0–0

Table 2
Interchain distances and interaction strengths for N02, N10, N12, N14 and N18.

Interchain distances calculated as the average of the limiting values at both ends of the overlapping tails $\{\Delta(\mathrm{T1,T2}) = \frac{1}{2}[d_1 + d_2]\}$. The reported dispersion is calculated as their difference $[\mathrm{abs}(d_1 - d_2)]$.

Compound	Δ(T1, T2) (Å)	AIM results	
		$\Sigma 100 \times \rho$†	$\Sigma 100 \times \nabla^2\rho$†
N02	N.a.	–	–
N10	4.85 (5)	4.2	1.4
N12	4.03 (3)	6.2	2.1
N14	3.99 (2)	7.5	2.5
N16	4.00 (3)	9.0	3.0
N18	3.95 (2)	10.5	3.5

† We report here the total sum of the 20–30 interactions between chains, with individual values ranging between 0.2–0.6 (for ρ) and 0.06–0.2. (for $\nabla^2\rho$).

showing that the shift takes place in the same plane of the tails and not perpendicular to them, as in the preceeding group. Table 2 presents a summary of interchain distances for the N10–N18 group.

In all cases, however, and due to their particular disposition, equivalent tails (through a [010] translation) define a nearly planar two-dimensional substructure of parallel chains, in a (100) orientation. These substructures are flanked by one hydrophobic (Pho) 'wall' made up of CH_3 groups, and a hydrophilic (Phi) one made up of aromatic heads with their protruding Br atoms. The weak C—H···O, C—H···π, C—Br···π interactions presented in Table 3 are internal to this zone and thus also **provide to its inner coherence [meaning?]**. These type of contacts are fairly common in supramolecular chemistry and do not deserve any particular explanation. There is in Zone B, however, a special type of interaction, the so-called halogen···halogen bonds (C—Br···Br—C in the present case), which are not so frequent and which might merit a brief introduction. There are essentially two commonly accepted types of these C—X···X—C interactions (X = any halogen), which, according to their geometric disposition, have historically been divided into type I and type II (Scheme 2). Even if type II Br···Br short contacts have been crystallographically considered over many years (Sarma & Desiraju, 1986, Reddy *et al.*, 2006), only recently they have been widely recognized as true halogen bonds, *i.e.* based on nucleophile–electrophile interactions (Metrangolo & Resnati, 2014; Politzer & Murray, 2013). Nowadays, they are considered as essentially arising from electrostatic attractions between the positive charge density on the σ-hole on one Br atom (*viz.* Br1 atom in Fig. 5, for example) and the negative charge density on the 'belt' on the other 'perpendicular' Br atom ($\mathrm{Br2^{ii}}$ on Fig. 5), although very small covalent components have also been discerned in some cases (Cavallo *et al.*, 2016; Raffo *et al.*, 2016; Capdevila-Cortada & Novoa, 2015).

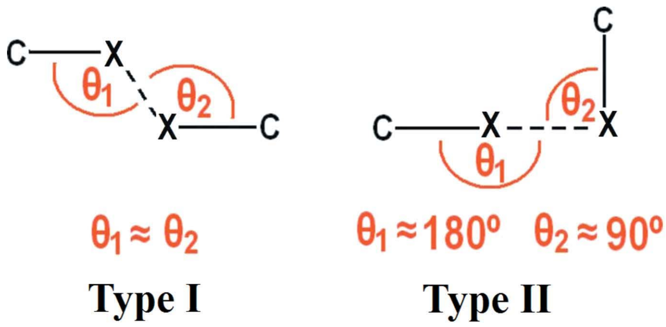

Scheme 1

Turning back to the analysis of Fig. 4, Zone B accounts for the mutual interaction between the latter hydrophilic 'walls', by way of Phi–Phi (Br···Br) contacts. There are two different Br···Br motives, common to the whole group where this interaction appears, and represented in Fig. 5(*b*) by the case N18, taken as representative: there is a centrosymmetric Br···Br interaction defining a head-to-head dimer, and a second, interdimeric one linking dimers laterally. Table 4 presents a detailed account of the Br···Br contacts: all of them fall into the 'type II' class of halogen–halogen bonds (Cavallo *et al.*, 2016; Gilday *et al.*, 2015; Reddy *et al.*, 2006), and their interactive character is apparent both from geometrical arguments [*viz.* all $d_{(\mathrm{Br\cdots Br})}$ distances lie within a few percent above/below the expected limiting value of 3.72 Å/twice the Br van der Waals radii, after Alvarez, 2013] as well as chemical considerations (*e.g.* they amply meet the

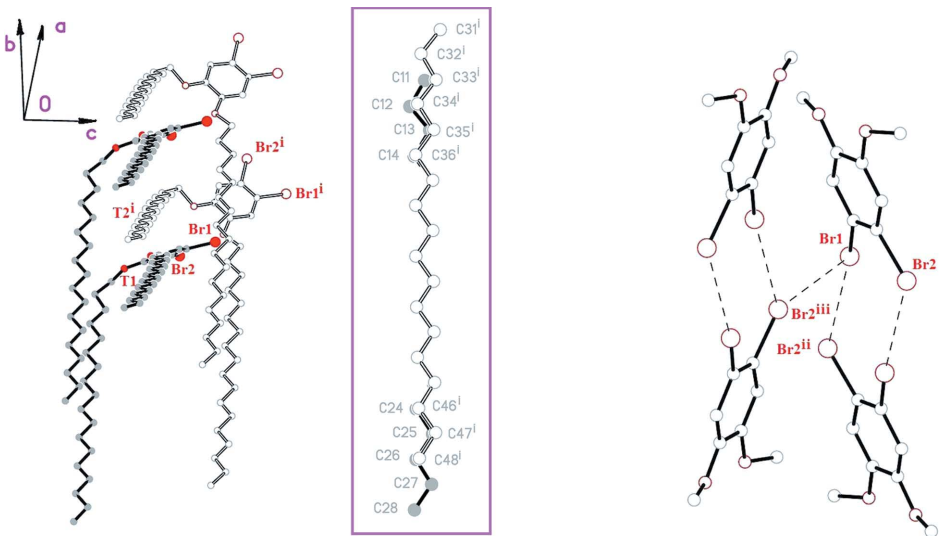

(*a*) (*b*)

Figure 5
(*a*) Schematic representation (for N18) of the disposition of the tails along *b*. Inset: projection along [010], disclosing the almost perfect superposition of the independent tails T1 and $\mathrm{T2^i}$: (i) $x, -2-y, \frac{1}{2}+z$. (*b*) The head-to-head interaction (N18, tails removed, for clarity) showing the two types of Br···Br interactions present. For detailed information on distances and symmetry codes see Table 4.

Table 3
C—H---O, C—H---π and C—Br---π interactions for N02, N10, N12, N14, N18 (Å, °).

						AIM results	
Structure	D—(H/Br)···A	D—(H/Br)	(H/Br)···A	D···A	D—(H/Br)···A	100 × ρ	100 × $\nabla^2\rho$
N02	C31—H31A---Cg1^{i}	0.97	2.81	3.614 (14)	142	–	–
	C1—Br1---Cg1^{ii}	1.88	3.913	4.798 (12)	106.5	0.39	0.10
N10	C7—H7A---Cg1^{iii}	0.97	3.046	3.874 (10)	143.9	0.35	0.08
	C6—Br1---Cg1^{iv}	1.89	4.183	5.530 (9)	126.8	–	–
N12	C32—H32B---Cg1^{v}	0.97	2.96	3.673 (8)	113	0.37	0.09
N14	C32—H32A---Cg1	0.97	2.96	3.678 (8)	131	0.37	0.09
N18	C11—H11A---O2	0.97	2.59	3.526 (11)	163	–	–
	C32—H32A---Cg1	0.97	2.95	3.650 (9)	130	0.38	0.10

Symmetry codes: (i) $x, -\frac{1}{2}-y, \frac{1}{2}+z$; (ii) $x, \frac{1}{2}-y, -\frac{1}{2}+z$; (iii) $\frac{1}{2}+x, \frac{1}{2}+y, z$; (iv) $\frac{1}{2}-x, \frac{1}{2}+y, -\frac{1}{2}-z$; (v) $x, \frac{3}{2}-y, -\frac{1}{2}+z$; (vi) $x, -\frac{1}{2}-x, \frac{1}{2}+z$; (vii) $x, 1-y, \frac{1}{2}+z$; (viii) $x, -y, -\frac{1}{2}+z$.

Table 4
Br···Br distances for N02, N10, N12, N14, N18 (Å).

				AIM results	
Compound	Br···Br	Dimeric	Interdimeric	100 × ρ	100 × $\nabla^2\rho$
N02	Br1···Br2^{i}	3.766 (3)	–	0.53	0.18
	Br1···Br2^{ii}	–	3.696 (3)	0.72	0.23
N10	Br1···Br2^{iii}	3.644 (3)	–	0.67	0.23
	Br2···Br2^{iii}	–	3.771 (3)	0.61	0.18
N12	Br1···Br2^{iv}	3.696 (3)	–	0.63	0.21
	Br2···Br2^{v}	–	3.745 (3)	0.49	0.15
N14	Br1···Br2^{vi}	3.707 (3)	–	0.61	0.21
	Br2···Br2^{vii}	–	3.736 (3)	0.50	0.18
N18	Br1···Br2^{viii}	3.675 (2)	–	0.66	0.22
	Br2···Br2^{ix}	–	3.687 (2)	0.63	0.20

Symmetry codes: (i) $1-x, -y, 1-z$; (ii) $1-x, \frac{1}{2}+y, \frac{3}{2}-z$; (iii) $\frac{1}{2}-x, \frac{1}{2}-y, 1-z$; (iv) $2-x, 1-y, 1-z$; (v) $2-x, -\frac{1}{2}+y, \frac{1}{2}-z$; (vi) $-x, -y, -1-z$; (vii) $-x, \frac{1}{2}+y, -\frac{1}{2}-z$; (viii) $\frac{1}{2}-x, \frac{1}{2}-y, 2-z$]; (ix) $\frac{1}{2}-x, \frac{1}{2}+y, \frac{3}{2}-z$.

chemical viewpoint suggested in Desiraju, 2013). Finally, Zone C corresponds basically to hydrophobic (Pho···Pho) methyl···methyl contacts.

The case of structure N16 departs somehow from what is discussed so far: the broad two-dimensional blocks defined by A organize themselves in a different manner, now head-to-tail in terms of molecular interactions, or Phi–Pho, in terms of hydrophilicity (labeled as B′ in Fig. 4).

4.2. Thermal behaviour and AIM analysis of the strength of the interactions

Melting points and enthalpies of the crystallized compounds have been measured by means of DSC experiments conducted on individual single crystals. Melting points (shown on Fig. 1) are essentially similar to those already reported for powdered samples (collected in Fonrouge *et al.*, 2013), also included in Fig. 1 as filled squares; the slightly higher values measured in our case, as well as the smoother curve we obtained, could arise from the fact that we have performed detailed DSC measurements under the same experimental conditions on individual single crystals, whereas reported values come from measurements performed by different research groups on powdered samples. The m.p. for N02 had not been reported previously. Its low value is likely related to the lack of significant intermolecular interactions; cohesion of the crystalline structure certainly arising from isotropic dispersion forces as the main contribution. The low value of its melting enthalpy (21 kJ mol^{-1}) agrees with this reasoning.

The m.p. of the higher homologues (N10–N18) of this series follow the trend already mentioned: as the chain length increases, the m.p. also increases. The usual interpretation detailed above, based on crystalline structures governed by the packing of the aliphatic chains, finds strong experimental support in the whole set of crystalline structures of N10, N12, N14, N16 and N18. In spite of the subtle differences found in both the space group and the interchain organization for N10 and in the 'head-to-tail' instead of a 'head-to-head' organization found for N16, all the crystalline structures are dominated by the organization of the aliphatic chains, as analyzed above.

Fig. 7(a) shows the measured melting enthalpies (ΔH_m) for the higher homologues of this series. As can be seen, ΔH_m increases linearly with n, with a small deviation for N16, whose ΔH_m value lies slightly below this straight line. The slope of 1.4 kJ mol^{-1} per added methylene is lower than the values found for the melting enthalpies of paraffins (Weast, 1975) – a fact already analyzed for long chain tails attached to rigid cores (Ibn-Elhaj *et al.*, 1992) – but close to that found for transition enthalpies of long-chain diruthenium pentacarboxylates, which also contain long aliphatic chains attached to rigid cores (Cukiernik *et al.*, 1998). This linear behavior is expected if the melting enthalpy represents the

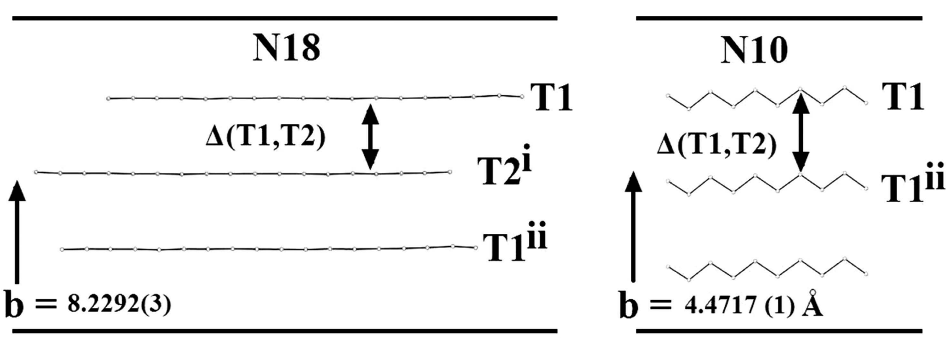

Figure 6
[001] projections of the tails (a) case N18, as representative of the N12–N18 group. (b) The N10 case. Symmetry codes: (i) $x, -2-y, \frac{1}{2}+z$; (ii) $x, 1+y, z$.

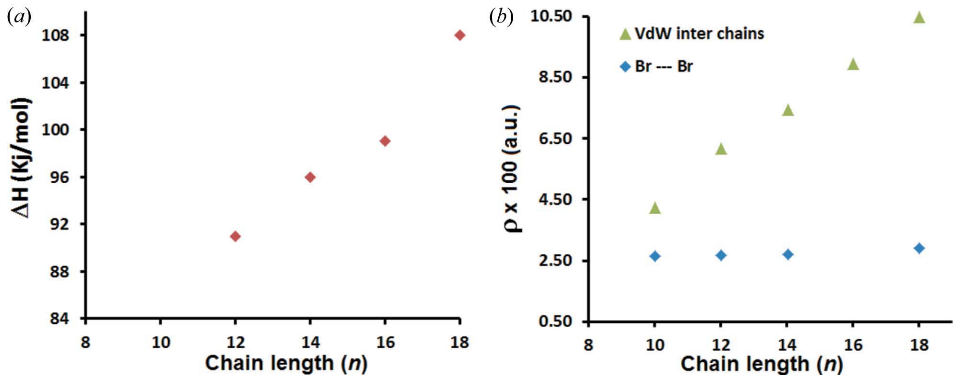

Figure 7
(*a*) Melting enthalpies (ΔH_m) as a function of n (number of C atoms in the tail). (*b*) Sum of (ρ) for interchain VdW (green) and Br···Br (blue) interactions *versus n*.

energy required to overcome the attractive interactions stabilizing the crystalline structure. Indeed, the narrow range spanned by the interatomic distances associated with these interactions in N10 to N18 suggests Br···Br and Br···*Cg* interactions of similar strength along the series; the melting enthalpy should then increase proportionally to n, reflecting the increase in van der Waals (VdW) interactions.

In order to understand the evolution of the strength of the interactions along the series beyond the level of the crystallographic analysis performed so far, based on geometric parameters alone, we have made use of AIM Bader's theory of Atoms in Molecules. In particular, we were interested in the comparison of the leading forces responsible for the packing in the 1,2-dibromo-4,5-dialkoxybenzenes family, *viz.* 'Br···Br' *versus* 'interchain van der Waals'. Individual values for the electron density and the Laplacian (determined as the sum of the eigenvalues of the Hessian of ρ) calculated at the bond critical points (BCP) of each of these interactions can be found as the two final columns in Tables 2 and 3 (Table S1 collects the corresponding values for all the interactions that might play a role along the N02–N18 series). As analyzed in the original paper by Bader (1991) these magnitudes of the electron density can be used as a measure of bond order and interaction strength. Inspection of Tables 2, 3 and S1 confirms the weak character of all the present interactions, with rather small values for (ρ) and ($\nabla^2\rho$) at the BCP comparable to those reported for similarly weak intermolecular hydrogen bonds (Koch & Popelier, 1995; Steiner, 2002; Wang *et al.*, 2016).

The total value of (ρ) for each of the two main interactions in each of the analyzed compounds is plotted against n in Fig. 7(*b*). As expected from its extensive character, the sum of (ρ) for the interchain VdW weak interactions increases steadily when the number of methylene groups in the chain increases, largely surpassing the strength of the Br···Br interactions, which remain fairly stable.

This analysis provides support to the qualitative interpretation given above for the linear behaviour of ΔH_m *versus* n. Moreover, the slightly low value of ΔH_m for N16 appears as additional proof of this interpretation, taking into account that this compound does exhibit VdW interchain interactions but not Br···Br interactions.

5. Conclusions

The crystalline structures of the four new members of the 1,2-dibromo-4,5-dialkoxybenzene series reported here provide further direct structural support for the 'diblock argument' usually invoked to explain the 'fall–rise' trends in the melting points of the homologous series. Contrary to our expectation, no transition from 'head-to-head' to 'head-to-tail' organization has been found for a given n value. Instead, the crystallographic analysis of the higher homologues (N10–N18) complemented with AIM and thermal analysis confirm that the main 'synthon' in the packing organization in the $n > 2$ group is the columnar array labeled as A in Fig. 4. The way in which cores interact (B or B′ in Fig. 4) would thus become a second-order effect subject to further, minor influences, and would explain an eventual departure (N16) from the general trend, as well as the subtly different way the tails pack in N10, a compound for which interchain VdW and Br···Br interactions seem to have closer energies than for the other memebers of this series.

Acknowledgements

We warmly thank Dr Pablo Albores (INQUIMAE) for the collection of the X-ray diffraction data of several crystals and for his interesting suggestions, Dr Matias Jobbagy (INQUIMAE) for his motivating comments at the beginning of this work as well as Drs Verónica E. Manzano (INQUIMAE) and Fabian Blanco (FCEN-UBA) for helping us with the synthesis of some of the reported compounds. We acknowledge ANPCyT (grant PME 01113) for an X-ray diffractometer, UBACyT (grant 20020130100776BA and undergraduate fellowships to AF and MEGS), CONICET (grant PIP 0659 and postdoctoral fellowship to SAS) and INQUIMAE (CSD license) for financial support. FDC is a member of the research staff of CONICET.

References

Alvarez, S. (2013). *Dalton Trans.* **42**, 8617–8636.
Bader, R. F. W. (1990). *Atoms in Molecules: A Quantum Theory.* Oxford University Press.
Bader, R. F. W. (1991). *Chem. Rev.* **91**, 893–928.
Bader, R. F. W. (2009). *J. Phys. Chem. A*, **113**, 10391–10396.
Bekö, S. L., Alig, E., Schmidt, M. U. & van de Streek, J. (2014). *IUCrJ*, **1**, 61–73.
Capdevila-Cortada, M. & Novoa, J. J. (2015). *CrystEngComm*, **17**, 3354–3365.
Cavallo, G., Metrangolo, P., Milani, R., Pilati, T., Priimagi, A., Resnati, G. & Terraneo, G. (2016). *Chem. Rev.* **116**, 2478–2601.
Cukiernik, F. D., Ibn-Elhaj, M., Chaia, Z., Marchon, J. C., Giroud-Godquin, A., Guillon, D., Skoulios, A. & Maldivi, P. (1998). *Chem. Mater.* **10**, 83–91.
Cukiernik, F. D., Zelcer, A., Garland, M. T. & Baggio, R. (2008). *Acta Cryst.* C**64**, o604–o608.

Demus, D., Goodby, J., Gray, G. W., Spiess, H.-W. & Vill, V. (1998). *Handbook of Liquid Crystals*, Vol. 1, pp. 133–187. Weinheim: Wiley-VCH.

Desiraju, G. R. (2002). *Acc. Chem. Res.* **35**, 565–573.

Desiraju, G. R. (2013). *J. Am. Chem. Soc.* **135**, 9952–9967.

Dunitz, J. D. & Gavezzotti, A. (1999). *Acc. Chem. Res.* **32**, 677–684.

Fonrouge, A., Cecchi, F., Alborés, P., Baggio, R. & Cukiernik, F. D. (2013). *Acta Cryst.* C**69**, 204–208.

Frisch, M. J. *et al.* (2009). *GAUSSIAN*09, Revision A.1. Gaussian, Inc., Wallingford, CT, USA.

Gilday, L. C., Robinson, S. W., Barendt, T. A., Langton, M. J., Mullaney, B. R. & Beer, P. D. (2015). *Chem. Rev.* **115**, 7118–7195.

Ibn-Elhaj, M., Guillon, D., Skoulios, A., Giroud-Godquin, A. M. & Maldivi, P. (1992). *Liq. Cryst.* **11**, 731–744.

Iwasaki, F., Yoshikawa, J. H., Yamamoto, H., Takada, K., Kan-nari, E., Yasui, M., Ishida, T. & Nogami, T. (1999). *Acta Cryst.* B**55**, 1057–1067.

Joseph, S., Sathishkumar, R., Mahapatra, S. & Desiraju, G. R. (2011). *Acta Cryst.* B**67**, 525–534.

Koch, U. & Popelier, P. L. A. (1995). *J. Phys. Chem.* **99**, 9747–9754.

Lu, T. & Chen, F. (2012). *J. Comput. Chem.* **33**, 580–592.

Martinez, C. R. & Iverson, B. L. (2012). *Chem. Sci.* **3**, 2191–2201.

Metrangolo, P. & Resnati, G. (2014). *IUCrJ*, **1**, 5–7.

Nishio, M. (2004). *CrystEngComm*, **6**, 130–158.

Oxford Diffraction (2009). *CrysAlisPro*, Version 171.33.48. Oxford Diffraction Ltd, Abingdon, Oxfordshire, England. **[replaced ref. by Wolff *et al.* which refers to *CrystalExplorer*]**

Platé, N. A. & Shibaev, V. P. (1974). *J. Polym. Sci. Macromol. Rev.* **8**, 117–253.

Politzer, P. & Murray, J. S. (2013). *ChemPhysChem*, **14**, 278–294.

Raffo, P. A., Marcolongo, J. P., Funes, A. V., Slep, L. D., Baggio, R. F. & Cukiernik, F. D. (2016). *J. Mol. Struct.* **1108**, 235–244.

Reddy, C. M., Kirchner, M. T., Gundakaram, R. C., Padmanabhan, K. A. & Desiraju, G. R. (2006). *Chem. Eur. J.* **12**, 2222–2234.

Rosokha, S. V., Stern, C. L. & Ritzert, J. T. (2013). *Chem. Eur. J.* **19**, 8774–8788.

Sarma, J. A. R. P. & Desiraju, G. R. (1986). *Acc. Chem. Res.* **19**, 222–228.

Sheldrick, G. M. (2008). *Acta Cryst.* A**64**, 112–122.

Sheldrick, G. M. (2015). *Acta Cryst.* C**71**, 3–8.

Spackman, M. (2015). *Cryst. Growth Des.* **15**, 5624–5628.

Steiner, T. (2002). *Angew. Chem. Int. Ed.* **41**, 48–76.

Wang, G., Chen, Z., Xu, Z., Wang, J., Yang, Y., Cai, T., Shi, J. & Zhu, W. (2016). *J. Phys. Chem. B*, **120**, 610–620.

Weast, R. C. (1975). Editor. *Handbook of Chemistry and Physics*, 56th ed, C-717–719. Boca Raton: CRC Press.

Acta Cryst B
STRUCTURAL SCIENCE
CRYSTAL ENGINEERING
MATERIALS

ISSN: 2052-5206

ORDER FORM

YOU WILL AUTOMATICALLY BE SENT DETAILS OF HOW TO DOWNLOAD AN ELECTRONIC REPRINT OF YOUR PAPER, FREE OF CHARGE. PRINTED REPRINTS MAY BE PURCHASED USING THIS FORM.

Please scan your order and send to jb@iucr.org

INTERNATIONAL UNION OF CRYSTALLOGRAPHY
5 Abbey Square
Chester CH1 2HU, England.

VAT No. GB 161 9034 76

Article No.: B160983-LO5009

Title of article Br· · ·Br and van der Waals interactions along a homologous series: crystal packing of 1,2-dibromo-4,5-dialkoxybenzenes

Name Ricardo F. Baggio

Address Gerencia de Investigación y Aplicaciones, Centro Atómico Constituyentes, Comisión Nacional de Energía Atómica, Buenos Aires, Argentina

E-mail address (for electronic reprints) baggio@tandar.cnea.gov.ar

OPEN ACCESS

IUCr journals offer authors the chance to make their articles open access on **Crystallography Journals** Online. For full details of our open-access policy, see http://journals.iucr.org/services/openaccess.html. For authors in European Union countries, VAT will be added to the open-access charge.

☐ I wish to make my article open access. The charge for making an article open access is **1200 United States dollars**.

DIGITAL PRINTED REPRINTS

I wish to order . . . . paid reprints

These reprints will be sent to the address given above. If the above address or e-mail address is not correct, please indicate an alternative:

PAYMENT

Charge for open access **1200** USD Charge for reprints . . . . USD Total charge . . . . USD

☐ A cheque for . . . . USD payable to **INTERNATIONAL UNION OF CRYSTALLOGRAPHY** is enclosed

☐ I have an open-access voucher to the value of . . . . USD Voucher No.

☐ An official purchase order made out to **INTERNATIONAL UNION OF CRYSTALLOGRAPHY** ☐ is enclosed ☐ will follow

Purchase order No.

☐ Please invoice me

☐ I wish to pay by credit card

EU authors only: VAT No:

Date | Signature

OPEN ACCESS

The charge for making an article open access is **1200 United States dollars**. For authors in European Union countries, VAT will be added to the open-access charge.

A paper may be made open access at any time after the proof stage on receipt of the appropriate payment. This includes all back articles on **Crystallography Journals Online**. For further details, please contact support@iucr.org. Likewise, organizations wishing to sponsor open-access publication of a series of articles or complete journal issues should contact support@iucr.org.

DIGITAL PRINTED REPRINTS

An electronic reprint is supplied free of charge.

Printed reprints without limit of number may be purchased at the prices given in the table below. The requirements of all joint authors, if any, and of their laboratories should be included in a single order, specifically ordered on the form overleaf. All orders for reprints must be submitted promptly.

Prices for reprints are given below in **United States dollars** and include postage.

	Size of paper (in printed pages)				
Number of reprints required	1–2	3–4	5–8	9–16	Additional 8's
50	184	268	372	560	246
100	278	402	556	842	370
150	368	534	740	1122	490
200	456	664	920	1400	610
Additional 50's	86	128	178	276	116

PAYMENT AND ORDERING

Cheques should be in **United States dollars** payable to **INTERNATIONAL UNION OF CRYSTALLOGRAPHY**. Official purchase orders should be made out to **INTERNATIONAL UNION OF CRYSTALLOGRAPHY**.

Orders should be returned by email to jb@iucr.org

ENQUIRIES

Enquiries concerning reprints should be sent to support@iucr.org.